VIRUS EVOLUTION

Virus Evolution, 2022, **8(2)**, 1–14

DOI: https://doi.org/10.1093/ve/veac059
Advance access publication date: 20 June 2022
Research Article

Defects in plant immunity modulate the rates and patterns of RNA virus evolution

Rebeca Navarro,[1,†,‡] Silvia Ambrós,[1,†,§] Anamarija Butković,[1,**,‡‡‡] José L. Carrasco,[1,††] Rubén González,[1,‡‡,§§§] Fernando Martínez,[1,§§] Beilei Wu,[1,***,****] and Santiago F. Elena[1,2,*,†††]

[1]Instituto de Biología Integrativa de Sistemas (CSIC—Universitat de València), Paterna, València 46182, Spain and [2]The Santa Fe Institute, Santa Fe, NM 87501, USA
[†]Equal contribution.
[‡]https://orcid.org/0000-0003-3263-6364
[§]https://orcid.org/0000-0003-3390-3102
[**]https://orcid.org/0000-0002-1435-0912
[††]https://orcid.org/0000-0002-5905-8042
[‡‡]https://orcid.org/0000-0001-9588-1127
[§§]https://orcid.org/0000-0001-6623-6858
[***]https://orcid.org/0000-0002-6141-4894
[†††]https://orcid.org/0000-0001-8249-5593
[‡‡‡]Current address: Institut Pasteur, 75015 Paris, France.
[§§§]Current address: Institut de Biologie de l'Ecole Normale Supérieure, CNRS, INSERM, 75005 Paris, France.
[****]Permanent address: Institute of Plant Protection, Chinese Academy of Agricultural Sciences, Haidian, 100193 Beijing, China.
*Correspondence author: E-mail: santiago.elena@csic.es

Abstract

It is assumed that host genetic variability for susceptibility to infection conditions virus evolution. Differences in host susceptibility can drive a virus to diversify into strains that track different defense alleles (e.g. antigenic diversity) or to infect only the most susceptible genotypes. Here, we have studied how variability in host defenses determines the evolutionary fate of a plant RNA virus. We performed evolution experiments with *Turnip mosaic potyvirus* in *Arabidopsis thaliana* mutants that had disruptions in infection-response signaling pathways or in genes whose products are essential for potyvirus infection. Plant genotypes were classified into five phenogroups according to their response to infection. We found that evolution proceeded faster in more restrictive hosts than in more permissive ones. Most of the phenotypic differences shown by the ancestral virus across host genotypes were removed after evolution, suggesting the combined action of selection and chance. When all evolved viral lineages were tested in all plant genotypes used in the experiments, we found compelling evidences that the most restrictive plant genotypes selected for more generalist viruses, while more permissive genotypes selected for more specialist viruses. Sequencing the genomes of the evolved viral lineages, we found that selection targeted the multifunctional genome-linked protein VPg in most host genotypes. Overall, this work illustrates how different host defenses modulate the rates and extent of virus evolution.

Key words: experimental evolution; generalism; plant immunity; plant-virus interactions; response to infection; specialization; virus evolution

1. Introduction

The spectrum of disease severity can be attributed to heterogeneity in virus virulence or host resistance and/or tolerance factors; the two are not necessarily independent explanations and they must actually complement and/or interact with each other resulting in an arms-race coevolutionary process. A common situation faced by viruses is that host populations consist of individuals that have different degrees of permissiveness to infection (Schmid-Hempel and Koella 1994; Pfenning 2001; Sallinen et al. 2020). Therefore, adaptive changes improving viral fitness in one host genotype may be selected against, or be neutral, in an alternative one. Genetic variability in the permissiveness of hosts and infectiousness of viruses have been well studied in animals and plants (e.g. Schmid-Hempel and Koella 1994; Altizer et al. 2006; Hughes and Boomsma 2006; Brown and Tellier 2011; Anttila et al. 2015; Parrat, Numminen, and Laine 2016; González, Butković, and Elena 2019; Sallinen et al. 2020). Theoretically, in the absence of host heterogeneity, parasites must evolve toward a host exploitation strategy that maximizes transmission with low virulence (Haraguchi and Sasaki 2000; Regoes, Nowak, and Bonhoeffer 2000; Rodríguez and Torres-Sorando 2001; Ganusov, Bergstrom, and Antia 2002; Gandon 2004; Lively 2010; Moreno-Gámez, Stephan, and Tellier 2013).

The interaction between host and parasite genotypes has been explained in the light of two different models that represent the two extremes on a continuum of possibilities. At one extreme the gene-for-gene model, in which a parasite genotype that can infect all host genotypes exists implies that a universally susceptible host genotype should also exist (Flor 1956). Resistance occurs when a host's *resistance* gene is matched by at least one parasite's *avirulence* gene. Polymorphism in permissiveness and infectivity can be maintained only if virulence pays a cost. At the other extreme, the matching-alleles model is based on self- versus nonself-recognition systems. Infection is not possible unless the parasite possesses all alleles that match those of the host (Frank 1993). In this case, polymorphisms are maintained by negative frequency-dependent selection. Along the continuum, variability in host defense mechanisms impacts the evolution of the parasite's virulence and other fitness-related traits. Viral infection of plants is a complex system in which the virus parasitizes the host and utilizes all its cellular resources to replicate and systemically spread. In response, plants have evolved intricate signaling mechanisms that limit the spread of the virus and result in resistance (Zhou and Zhang 2020). Broadly speaking, these factors can be classified into *basal* if they are preexisting and limit within-cell propagation and cell-to-cell spread and *inducible* if they are only activated upon infection and inhibit systemic virus movement and replication. Basal mechanisms include susceptibility (S) genes that involve alleles of cellular proteins that do not interact properly with viral factors, e.g. translation initiation factors required by the virus for successful exploitation of the cell's protein synthesis machinery, heat shock proteins that assist the formation of multiprotein complexes, or DNA-binding phosphatases (Carr, Lewsey, and Palukaitis 2010; Mäkinen 2019). In contrast, inducible mechanisms include genes whose expression results in a broad-scale change in plant physiology via diverse signal transduction pathways, particularly those regulated by the hormones salicylic acid (SA), jasmonic acid (JA), and ethylene (ET) (Soosaar, Burch-Smith, and Dinesh-Kumar 2005; Carr, Lewsey, and Palukaitis 2010). These changes include local cell apoptosis (Loebenstein 2009), the upregulation of nonspecific responses against many different types of pathogens throughout the entire plant (systemic acquired resistance—SAR and induced systemic resistance—ISR) (Kachroo, Chandra-Shekara, and Klessig 2006; Carr, Lewsey, and Palukaitis 2010), and the activation of the RNA-silencing-based resistance, that seems to play a role both in basal and inducible mechanisms (Voinnet 2001; Carr, Lewsey, and Palukaitis 2010). Early host responses following virus detection include changes in ion fluxes (mainly Ca^{++}), activation of signaling pathways, major alterations of transcriptomic profiles, generation of reactive oxygen species, and production of nitric oxide (Soosaar, Burch-Smith, and Dinesh-Kumar 2005). These immediate changes are followed by cell apoptosis and the recruitment of SA and JA/ET signaling pathways. The SA-mediated defense signaling pathway results in SAR, while the JA/ET-mediated defense signaling pathway results in ISR, the latter being specifically involved in interactions between plants and beneficial microbes. Indeed, it appears that ISR is not effective against most viruses (Ton et al. 2002; Loebenstein 2009; Pieterse et al. 2009). Both SAR and ISR pathways converge into two master regulator genes, the *ENHANCED DISEASE SUSCEPTIBILITY 1* (*EDS1*) and the *PHYTOALEXIN DEFICIENT 4* (*PAD4*). *EDS1* and *PAD4* repress ISR and promote SAR. Although the SA and JA/ET pathways have been viewed as mutually antagonistic, several studies have revealed positive and negative crosstalk between them (Van Wees et al. 2000; Pieterse et al. 2012) as well as with the RNA-silencing pathway (Soosaar, Burch-Smith, and Dinesh-Kumar 2005; Carr, Lewsey, and Palukaitis 2010; Yang et al. 2020). This crosstalk shows the topological structure of an incoherent feed-forward loop that confers robustness and tunability to the plant immune network (Mine et al. 2017).

Here we have used the turnip mosaic virus (TuMV; species *Turnip mosaic potyvirus*, genus *Potyvirus*, family *Potyviridae*)—*Arabidopsis thaliana* experimental pathosystem to explore how defects in basal and inducible defenses affect virus evolution. After exploring the variability of phenotypic responses to TuMV infection in a collection of twenty-one *A. thaliana* genotypes, ten of them were chosen, covering a wide spectrum of host phenotypic responses. Then, we performed virus evolution experiments on each of these genotypes and tracked the evolution of quantitative disease-related traits. At the end of the evolution experiment, we evaluated the effects of host genotypes in the extent of observed phenotypic changes, rates of virus evolution and the contribution of historical contingency, selection and stochasticity in the outcome of evolution. Next, we explored whether different TuMV lineages evolved as more specialist or more generalists depending on the disrupted defense mechanism in their local host. Finally, we identified the pattern of molecular changes in the genomes of the different viral lineages.

2. Materials and methods

2.1 Plants, viruses, and growth conditions

A collection of twenty-one different *A. thaliana* (L.) Heynh genotypes of the Col-0 accession were used for this study Table 1. This collection covered a wide range of possible resistance mechanisms. None of them showed a strong deleterious phenotype that might later interfere with the identification of infection symptoms. In all experiments described below, plants were maintained in a BSL2 climatic chamber under a photoperiod of 8-h light (LED tubes at PAR 90–100 $\mu mol/m^2/s$) at 24°C and 16-h dark at 20°C and 40 per cent relative humidity.

TuMV infectious sap was obtained from TuMV-infected *Nicotiana benthamiana* Domin plants inoculated with the infectious plasmid p35STunos containing a cDNA of the TuMV genome (GeneBank accession AF530055.2) under the control of the cauliflower mosaic virus 35S promoter and the *nos* terminator (Chen et al. 2003) as described elsewhere (González, Butković, and Elena 2019; Corrêa et al. 2020). This TuMV sequence variant corresponds to the YC5 strain from calla lily (*Zantesdeschia* sp.) (Chen et al. 2003). After plants showed symptoms of infection, they were pooled and frozen with liquid N_2. This frozen plant tissue was homogenized into a fine powder using a Mixer Mill MM400 (Retsch GmbH, Haan, Germany). For inoculations, 0.1 g of powder was diluted in 1 ml inoculation buffer (50 mM phosphate buffer pH 7.0, 3 per cent PEG6000, 10 per cent Carborundum) and 5 µl of the inoculum was gently rubbed onto two leaves per plant. Plants were all inoculated when they reached growth stage 3.5 in the Boyes et al. (2001) scale. This synchronization ensures that all hosts were at the same phenological stage when inoculated.

2.2 Phenotyping infection

Five different disease-related traits were measured for each infected plant ($n = 20$) during 15 days postinoculation (dpi): (1) change in dry weight of the aerial part of infected plants, with a precision of 10 mg, relative to the corresponding noninfected controls (Supplementary Fig. S1A). (2) Severity of symptoms evaluated

Table 1. Different *A. thaliana* genotypes used in this study. Highlighted in gray are those used for the evolution experiments.

Genotype	Gene name	Affected pathway	Expected phenotype relative to wildtype plants	Reference
Wildtype				
coi1-4	*CORONATINE INSENSITIVE 1* (AT2G39940)	Repression of JA-responsive genes	No ISR, no effect on virus	Thines et al. (2007)
cpr5-2	*CONSTITUTIVE EXPRESSOR OF PR GENES 5* (AT5G64930)	Membrane protein, negative regulator of pathogen-dependent SA signaling	More resistant, constitutive SAR	Love et al. (2007)
dbp2	*DNA-BINDING PROTEIN PHOSPHATASE 2*	Transcriptional regulation of gene expression in potyvirus-infected plants	More resistant to potyvirus infection	Castelló et al. (2011)
dcl2	*DICER-LIKE 2* (AT3G03300)	Partial loss of RNA-silencing	No effect, siRNAs produced by DCL4	Bouché et al. (2006)
dcl4	*DICER-LIKE 4* (AT5G20320)	Partial loss of RNA-silencing	No effect, siRNA produced by DCL2	Bouché et al. (2006)
dcl2 dcl4	Double mutant *dcl2 dcl4*	Complete loss of RNA-silencing	More susceptible, no siRNA production	Bouché et al. (2006)
dip2	*DBP-INTERACTING PROTEIN 2* (AT5G03210)	Transcriptional regulation of gene expression in potyvirus-infected plants	More susceptible	Castelló et al. (2011)
eds4-1	*ENHANCED DISEASE SUSCEPTIBILITY 4* (AT5G51200)	Loss of SA-dependent signaling	More susceptible, no SAR	Gupta, Willits, and Glazebrook (2000)
eds5-1	*ENHANCED DISEASE SUSCEPTIBILITY 5* (AT4G39030)	Lipase-like protein, positive regulator of pathogen-dependent SA signaling	More susceptible, no SAR	Nawrath et al. (2002)
eds8-1	*ENHANCED DISEASE SUSCEPTIBILITY 8*	Reduced expression of plant defensin genes, reduced ISR	More resistant, enhanced SAR	Love et al. (2007)
ein2-1	*ETHYLENE INSENSITIVE 2* (AT5G03280)	MAPK, ET signaling intermediate, negative regulator SA-dependent signaling	More resistant, enhanced SAR	Love et al. (2007)
etr1-1	*ETHYLENE RESPONSE 1* (AT1G66340)	ET receptor, negative regulator SA-dependent signaling	More resistant, enhanced SAR	Love et al. (2007)
hsp90-1	*HEAT SHOCK PROTEIN 1* (AT5G52640)	Recessive *r* gene, required for membrane-bound replication complexes; protein folding	More resistant, missing component for viral replication	Verchot (2012)
i4g1	*EUKARYOTIC TRANSLATION INITIATION FACTOR (ISO) 4 G 1* (AT3G60240)	Recessive *r* gene, initiation of viral RNA translation	More resistant, missing component for viral gene expression	Nicaise et al. (2007)
i4g2	*EUKARYOTIC TRANSLATION INITIATION FACTOR (ISO) 4 G 2*	Recessive *r* gene, initiation of viral RNA translation	More resistant, missing component for viral gene expression	Nicaise et al. (2007)
jin1	*JASMONATE INSENSITIVE 1* (AT1G32640)	Loss of JA signaling; negative regulator of SA-dependent signaling	More resistant, enhanced SAR	Laurie-Berry et al. (2006)
npr1-1	*NONEXPRESSER OF PR GENES 1* (AT1G64280)	Ankyrin-repeat protein required for *PR-1* activation	More susceptible, no SAR, no ISR	Cao et al. (1994)
$p58^{IPK}$	*HOMOLOG OF MAMMALIAN* $P58^{IPK}$ (AT5G03160)	Constitutive activation of PKR	More resistant, strong apoptosis-mediated HR	Bilgin et al. (2003)
pad4-1	*PHYTOALEXIN DEFICIENT 4* (AT3G52430)	Lipase-like protein, positive regulator pathogen-dependent SA signaling	More susceptible, no SAR	Cui et al. (2018)
sid2-1	*SA INDUCTION DEFICIENT 2* (AT1G74710)	Isochorismate synthase, required for SA bioshynthesis	More susceptible, no SAR	Nawrath and Métraux (1999)

ET—ethylene; HR—hypersensitive response; ISR—induced systemic resistance; JA—jasmonic acid; MAPK—mitogen-activated protein kinase; PKR—protein kinase RNA-activated; SA—salicylic acid; SAR—systemic acquired resistance.

in a semiquantitative discrete scale (as shown in Fig. 1B in Corrêa et al. 2020) ranging from zero for non-infection or asymptomatic infections to four for plants showing a generalized necrosis and wilting (Supplementary Fig. S1B). (3) The area under the disease progress stairs (*AUDPS*) (Supplementary Fig. S1C) takes values in the range (0, *N*) where *N* is the total number of days included in the assay (Simko and Piepho 2012). *AUDPS* is a good metric for pathogenicity and transmission efficiency, as it summarizes the number of infected individuals as well as the temporal dynamics at which symptoms appear in the host population into a single figure (Jeger and Viljanen-Rollinson 2001; Simko and Piepho 2012; Alves and Del Ponte 2021). (4) Permissiveness to infection measured as the frequency of symptomatic plants out of the number of inoculated plants at 15 dpi (Supplementary Fig. S1D) and (5) viral load measured by absolute reverse transcription real-time quantitiative polymerase chain reaction (RT-qPCR) as the number of viral genomes per ng of total RNA in the plant as described below (Supplementary Fig. S1E).

Plant genotypes were clustered according to their phenotypic similarity in response to TuMV infection using a nearest-neighbor clustering algorithm and the multivariate Euclidean distance. The optimal number of clusters was confirmed by a *k*-means classification method using the minimum value of Bayes information criterion (*BIC*) among a set of competing models.

2.3 Experimental evolution

Five TuMV lineages were evolved during twelve consecutive serial passages in each one of the nine selected mutant genotypes. In

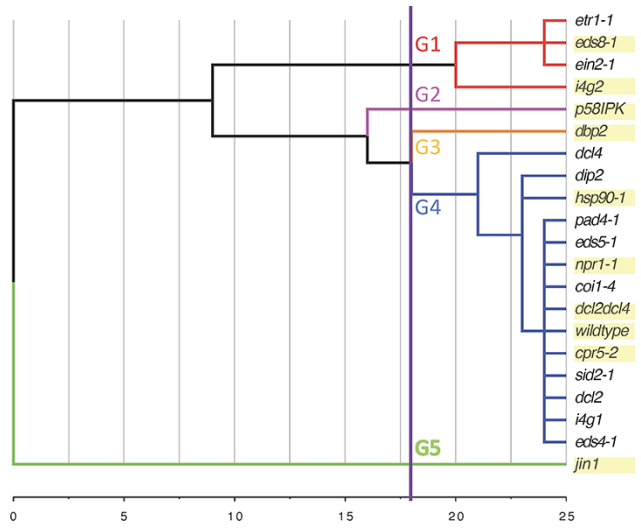

Figure 1. Nearest-neighbor clustering of the twenty-one genotypes of *A. thaliana*. Based on the squared Euclidean distance among multivariate vectors of phenotypic traits in response to TuMV infection. Genotypes selected as hosts for the evolution experiments are highlighted . The thick vertical line represents the cutoff criteria used to define the statistically significant phenogroups (lowest *BIC* value was obtained for five phenogroups G1 to G5).

addition, two lineages were also evolved in wild type (WT) plants. To begin the evolution experiment, ten *A. thaliana* plants at developmental stage 3.5 in Boyes et al. (2001) scale per lineage and genotype were inoculated as described above with the virus stock previously generated from infected *N. benthamiana* plants inoculated with infectious clone p35STunos. The next passages were made by harvesting the symptomatic plants at 12 dpi, preparing the infectious sap as described above, and inoculating it to a new healthy population of ten plants.

2.4 Total RNA extractions and quantification of viral load

Pools were made of ten infected symptomatic plants per lineage, genotype, and serial passage, frozen with liquid N_2 and preserved at –80°C until it was homogenized into fine powder. Next, aliquots of approximately 0.1 g of grounded tissues were used for total RNA (RNAt) extractions. The RNAt was extracted with the Agilent Plant RNA isolation Mini kit (Agilent Technologies, Santa Clara CA, USA). Three aliquots of RNAt per each sample were separated and their concentration adjusted at approximately 50 ng/μl to estimate viral load.

Viral load was quantified in each of the three aliquots by absolute real-time quantitative RT-PCR (RT-qPCR) using standard curves and the primers TuMV F117 forward (5′-CAATACGTGCGAG AGAAGCACAC-3′) and F118 reverse (5′-TAACCCCTTAACGCCAA GTAAG-3′) that amplify a 173 nucleotides fragment from the *CP* cistron of TuMV genome, as previously described (Corrêa et al. 2020). Briefly, standard curves were constructed using ten serial dilutions of the TuMV genome, that was synthesized by *in vitro* transcription as detailed previously (Cervera et al. 2018), in RNAt extract obtained from healthy *A. thaliana* plants used as control in the experiments. Amplification reactions were run in a 20 μl volume using the GoTaq 1-Step RT-qPCR System (Promega, Madison WI, USA) and the recommended manufacturer's instructions in an ABI StepOne Plus Real-time PCR System (Applied Biosystems, Foster City CA, USA). The cycling conditions consisted of an RT phase of 5 min at 42°C and 10 min at 95°C followed by a PCR stage consisting of 40 cycles of 5 s at 95°C and 34 s at 60°C, and the final melt curve profile that consisted of 15 s at 95°C, 1 min at 60°C and 15 s at 95°C. Negative controls consisted of healthy RNAt plant extract (mock-inoculated noninfected control) and water. For each sample, three technical replicates were quantified. The results were analyzed using the StepOne software 2.2.2 (Applied Biosystems).

2.5 TuMV genome amplifications and sequencing

A sample of the above RNAt obtained at passage 12 from each viral lineage was used to generate the viral consensus sequence. RNAs were amplified by high-fidelity RT-PCR using the AccuScript Hi-Fi (Agilent Technologies) reverse transcriptase and Phusion DNA polymerase (Thermo Scientific, Waltham MA, USA) following the manufacturer's instructions. Each complete TuMV genome was amplified into three overlapping amplicons of 3114 (5′ fragment R1), 3697 (central region R2), and 3287 nucleotides (3′ fragment R3) using three primer sets. For RT reactions an aliquot of the corresponding RNAt (150–300 ng) was mixed with 0.25 μM of the 1 R-P3 (5′-CGAGTAGTATCTTATAGCACAGCGCTCCGACC-3′), 2 R-NIa (5′-TGTCTGGAATCGGTAGCAAATGTAGCTGAGTTGTG-3′) or 3 R-polyAR (5′-TTTTTTTTTTTTTTTTTTTTTGTCCCTTGCATCAT ATCAAATG-3′) primer to synthesize the R1, R2 or R3 cDNA fragment, respectively, that were denatured 5 min at 65°C and cooled on ice. Then a mix containing AccuScript Hi-Fi 1× Buffer, 1 mM of dNTPs, 8 mM of DTT, 4 U of Ribolock RNase inhibitor (Thermo Scientific), and 0.5 μl of AccuScript Hi-Fi (Agilent Technologies) was added up to a 10 μl volume. RT reactions consisted of 90 min at 42°C to synthesize the cDNA followed by an incubation of 5 min at 70°C to inactivate the enzyme. PCR reactions were performed in a 50 μl volume containing a mix of 1× Phusion Buffer, 0.4 μM of dNTPs, 0.2 μM of each primer, 0.5–1 μl of DMSO, 2U of Phusion DNA polymerase (Thermo Scientific), and 1 μl of the corresponding RT reaction. R1 fragment was amplified using the primer set 1F-5UTR (5′-GCAAACGCAGACCTTTCGAAGCACTCAAGC-3′) and 1R-P3 and the following PCR conditions: an initial denaturation of 30 s at 98°C, 3 cycles of 10 s at 98°C, 20 s at 67°C and 2 min at 72°C, 3 cycles of 10 s at 98°C, 20 s at 65°C and 2 min at 72°C, and 32 cycles of 10 s at 98°C, 20 s at 63°C and 2 min at 72°C, followed by a final extension step of 5 min at 72°C. Fragments R2 and R3 were amplified with primer set 2F-P3 (5′-TGGGAGCTTGCGGATGGTGGATACACAATTC-3′) and 2R-NIa or 3F-NIa (5′-CTCGTTATATGGAGTCGGTTTCGGACCACTCATAT-3′) and 3R-polyAR, respectively and a PCR with the same denaturation and extension steps than the fragment R1 but different amplification steps: a stage consisting of 15 cycles of 10 s at 98°C, 20 s at 67°C, and 2 min at 72°C followed by 23 cycles of 10 s at 98°C, 20 s at 65°C, and 2 min at 72°C for fragment R2. For fragment R3, 15 cycles of 10 s at 98°C, 20 s at 67°C, and 2 min at 72°C followed by 23 cycles of 10 s at 98°C, 20 s at 65°C, and 2 min at 72°C were used. PCR products were purified with the MSB Spin PCRapace Kit (Stratec Molecular, Coronado CA, USA) and then Sanger-sequenced. Full-length consensus viral sequences were obtained assembling the sequences of the three amplified products by using the Genious R9.0.2 program.

2.6 Statistical analyses

AUDPS data were fitted to an analysis of variance (ANOVA) model with plant genotype (*G*) as main factor, independent evolution lineages (*L*) were nested within *G* and passage (*t*) was introduced in the model as a covariable. The full model equation thus reads:

$$AUDPS_{ijk}(t) \sim A + t + G_i + L(G)_{ij} + (t \times G)_i + [t \times L(G)]_{ij} + \varepsilon_{ijk} \quad (1)$$

where $AUDPS_{ijk}(t)$ is the value observed at time t, for an individual infected plant k of evolutionary lineage j of genotype i, A represents the grand mean value and ε_{ijk} stands for the error assumed to be Gaussian distributed at every t. The type III sum of squares was used to partition total variance among factors. The magnitude of the effects was evaluated using the η_P^2 statistic (proportion of total variability in *AUDPS* attributable to each factor in the model; conventionally, values of $\eta_P^2 \geq 0.15$ are considered as large effects).

To test the relative contribution of selection, chance, and historical contingency in the outcome of the evolutionary process, the statistical approach described by Travisano et al. (1995) has been used. One can imagine two situations. Firstly, ancestral biological differences among phenotypes could be preserved during evolution despite a net increase in the mean trait values (due to selection) and differences among replicated lineages (due to chance; i.e. mutation and drift). In this situation, we should expect a nonzero slope in a regression of the evolved phenotypic values against the ancestral ones. The closer the slope to ≈ 1, the greater the importance of ancestral differences. Secondly, if initial trait variation among ancestral genotypes was eliminated from the evolved populations because the combined effect of adaptation and chance, we should expect a regression slope < 1. The lesser the effect of ancestral differences, the flatter the slope, being zero in the extreme case where ancestral differences have been completely erased. The estimated slope of the regression of the evolved phenotypic values against the ancestral ones was obtained by least-squares linear regression. The estimated slopes were compared against the slope expected under the null hypothesis of ancestral differences being fully conserved (*i.e.* 1) using one-sample *t*-tests.

Rates of phenotypic evolution for *AUDPS* were estimated by fitting the time series data to a power-law model of fitness evolution in asexual populations (Wiser, Ribeck, and Lenski 2013) using the Levenberg–Marquardt nonlinear minimum squares regression method. The model equation fitted has the form:

$$AUDPS(t) = [AUDPS(0) + at]^{1/b} \quad (2)$$

where $AUDPS(k)$ represents the *AUPDS* value at passage k, and a and $b > 0$ are parameters that summarize properties of the distribution of beneficial mutations, their average time to fixation, and the intensity of clonal interference (Wiser, Ribeck, and Lenski 2013). Interestingly, it is possible to evaluate the maximum rate of *AUDPS* evolution, v, at the beginning of the evolution experiment as:

$$v = \lim_{t \to 0} \frac{dAUDPS(t)}{dt} = \frac{a}{b} \quad (3)$$

All the statistical analyses described were done with SPSS version 27 software (IBM, Armonk, NY) otherwise indicated.

2.7 Analysis of infection network

An infection matrix was estimated in a single experimental block in which all evolved viral lineages were inoculated in all mutant genotypes, ten plants per combination. *AUDPS* was estimated for each viral lineage—host genotype combination as described above.

The resulting infection matrix was analyzed using tools borrowed from the field of network biology to explore whether they show random associations between viral lineages and host genotypes, one-to-one associations, nestedness indicative of a gene-for-gene type of interaction, or modularity (Weitz et al. 2013). The statistical properties of the infection matrix were evaluated using the R package 'bipartite' version 2.15 (Dormann and Strauss 2014) in R version 4.0.0 under RStudio 1.2.1335. Four different summary statistics were evaluated: *T* nestedness (Bascompte et al. 2003), Q modularity (Newman 2006) and the *d'* species-level (or Kullback-Leibler divergence) and H_2' network-level (or two-dimensional normalized Shannon entropy) specialization indexes (Blüthgen, Menzel, and Blüthgen 2006). Both *d'* and H_2' range between zero and one for extreme generalists and specialists, respectively. The statistical significance of these statistics was evaluated using Bascompte et al. (2003) null model. Readers interested in mathematical details, please see Mariani et al. (2019) for *T* and Q definitions and Blüthgen, Menzel, and Blüthgen (2006) for *d'* and H_2'.

Previous to these analyses, *AUDPS* data were binned into ten intervals of equal size with bounds

$$\left[AUDPS_{min} + \frac{i}{10}(AUDPS_{max} - AUDPS_{min}), AUDPS_{min} + \frac{(i+1)}{10}(AUDPS_{max} - AUDPS_{min})\right]$$

where $i \in [0, 9]$, as described in Moury et al. (2021).

2.8 The statistics of molecular evolution

Treating each lineage as an observation and each host genotype as a subpopulation, we evaluated the average nucleotide diversity within-host genotypes, π_S, the nucleotide diversity for the entire sample, π_T, the interhost genotypes nucleotide diversity, δ_{ST}, and the estimate of the proportion of interhost genotypes nucleotide diversity, known as coefficient of nucleotide differentiation (Nei 1982), $N_{ST} = \delta_{ST}/\pi_T$. Standard deviations of estimates were inferred from 1,000 bootstrap samples. All these computations were done using MEGA 11 (Tamura, Stecher, and Kumar 2021) and the lowest-*BIC* nucleotide substitution model Kimura 2-parameters (Kimura 1980). Tajima's *D* test of selection (Tajima 1989) and its statistical significance were evaluated using DnaSP6 (Rozas et al. 2017).

The frequency of mutations (m) per cistron (C), relative to the length of the corresponding cistron, was fitted to the following logistic regression model using generalized linear model techniques with a binomial probability distribution and a probit link function:

$$\text{probit}(m_i) \sim \mu + C_i + \varepsilon_i \quad (4)$$

where μ is the average genomic mutation frequency and i refers to the ten cistrons in the main open reading frame.

3. Results

3.1 Classification of plant genotypes according to the phenotype of TuMV infection

The twenty-one *A. thaliana* genotypes used in this study are shown in Table 1, including information about the affected signaling pathways or cellular processes as well as the expected phenotype of infection relative to WT plants. Genotypes were classified according to the phenotype of TuMV infection based on the five different disease-related traits described in Section 2.2. In order to classify plant genotypes according to their similarity in phenotypic response to TuMV infection, a nearest-neighbor clustering was obtained Fig. 1. We found five significant phenogroups that also minimized the *BIC* in a *k*-means analysis [$BIC(5) = 12.241$ compared to $BIC(4) = 15.668$ and $BIC(6) = 18.249$]. Hereafter, we will refer to them as phenogroups G1 to G5. The characterization of the phenotypic differences among these groups is presented in the Supplementary Text S1 and Figs. S1 and S2. In short, the

members of phenogroup G1 show enhanced restriction to TuMV infection. The only member of phenogroup G2 ($p58^{IPK}$) shows no significant changes in *AUDPS*, infectivity, symptoms severity, and viral load relative to infected WT plants but a strong reduction in the change in dry weight. The only member of phenogroup G3 (*dbp2*) also shows enhanced restriction although without significant reduction in viral load. G4 represents a sort of hodgepodge formed by genotypes that do not show a clear phenotypic difference from WT Fig. 1. The only member of phenogroup G5 (*jin1*) shows a significant increase in all measured traits except viral load.

Representatives from the five phenogroups were randomly selected for the subsequent evolution experiment (shadowed rows in Table 1): *eds8-1* and *i4g2* from phenogroup G1 representing the more restrictive genotypes; $p58^{IPK}$ from G2; *dbp2* from G3; *cpr5-2*, *dcl2 dcl4*, *hsp90-1*, *npr1-1*, and WT from G4; and *jin1* from G5 representing the more permissive genotype.

3.2 Experimental TuMV evolution in plants from each phenogroup

First, we sought to evaluate the dynamics of evolution for *AUDPS* Fig. 2. Recall that in our experiments, only viruses evolved while plants did not, so changes in infection phenotypes were due to the evolution of viruses and the way they interact with plants. Notice that lineage *cpr5-2/L2* showed quite a different evolution pattern from the other four lineages evolved in *cpr5-2*. It never increased in *AUDPS* and was lost after passage five Fig. 2. Therefore, we ended up with a total of forty-six evolved lineages.

Data were fitted into the ANOVA model described in Eq. 1 of Section 2.6. Despite a considerable amount of noise in the time series, we found some significant results that can be summarized as follows Table 2. First, a net significant and large ($\eta^2_P = 0.399$) effect associated with the evolutionary passages (t term in Eq. 1) has been observed, indicating that *AUDPS* evolved during the experiment. Second, plant genotypes (G term in Eq. 1) had a highly significant and very large ($\eta^2_P = 0.868$) effect on the phenotypic traits, suggesting that TuMV evolutionary dynamics were strongly influenced by the local host genotype in which it was being passaged. Third, independent lineages evolved in the same host genotype show a high degree of parallelism, as indicated by a nonsignificant lineage effect [$L(G)$ term in Eq. 1, with $\eta^2_P = 0.029$; and term $t \times L(G)$ in Eq. 1, with $\eta^2_P = 0.039$].

To evaluate the role of the ancestral differences (Travisano et al. 1995) in the evolution of *AUDPS* across the ten plant genotypes, we evaluated the magnitude of their change at the end of the evolution experiment. Fig. 3A shows the plots of evolved *vs* ancestral values. For illustrative purposes, the solid red line represents the null hypothesis of absolute preservation of ancestral differences. A significant regression exists between evolved and ancestral values ($R = 0.491$, $F_{1,44} = 14.000$, $P < 0.001$), with slope 0.284 ± 0.076 (± 1 SD). Since the slope is still significantly different from zero, yet clearly flatter than the expected relationship of slope one ($t_{44} = 9.422$, $P < 0.001$), we concluded that ancestral differences have been mostly removed by the combined action of selection and chance, yet not completely erased.

3.3 Rates of *AUDPS* evolution

To explore the possible impact of different plant immunity mechanisms on the rates of virus phenotypic evolution, we estimated the rates of *AUDPS* evolution using the power-law model described by Eq. 2 in Section 2.6.

Fig. 3B shows the estimated rates of evolution for host genotypes ordered from the most restrictive (phenogroup G1) to the most permissive (phenogroup G5). Very interestingly, the regression coefficient was significantly negative ($-6.394 \cdot 10^{-4} \pm 2.843 \cdot 10^{-4}$; $R = 0.321$, $F_{1,44} = 5.061$, $P = 0.030$), suggesting that evolution proceeded faster in the most restrictive hosts and slower in the most permissive ones.

In conclusion from this section, we found that differences in the maximum rates of evolution at the beginning of the evolution experiment between permissive and resistant hosts actually depend on the particular resistance mechanism.

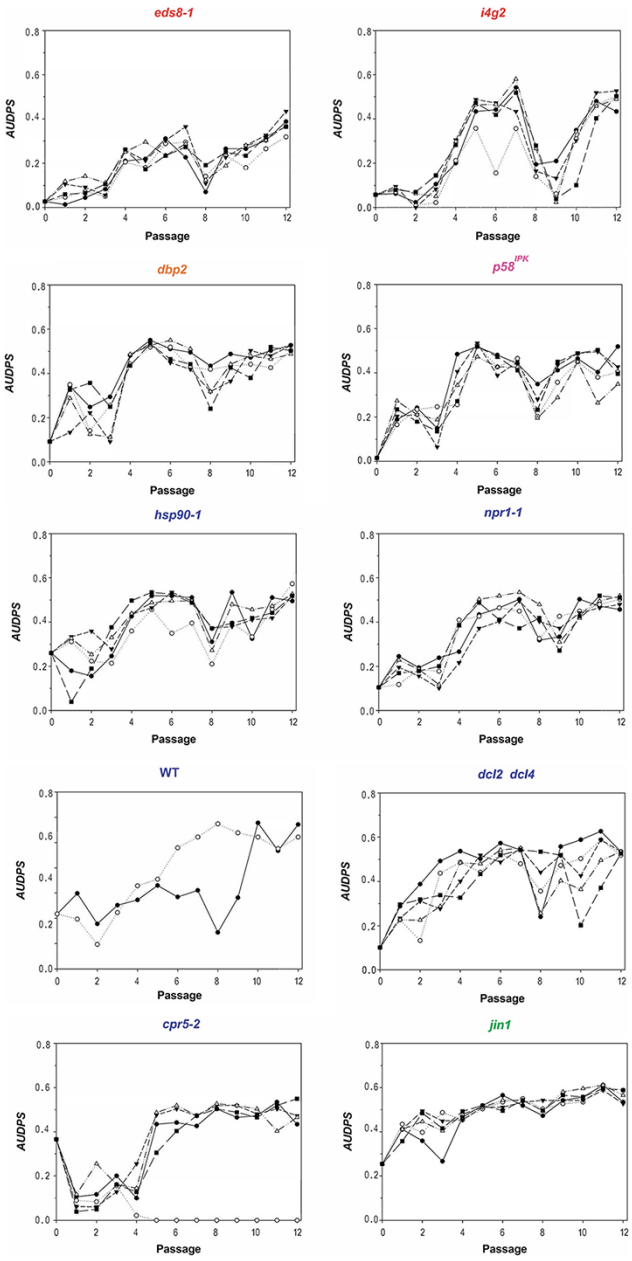

Figure 2. Evolution of *AUDPS* along the passages of experimental evolution on each different host genotype. Different symbols and lines represent the independent evolutionary lineages. Panels are arranged from the most resistant genotype (*eds8-1*) to the most sensitive one (*jin1*) according to the phenogroups defined in Fig. 1 and colored using the same palette.

Table 2. Results of the ANOVA model for *AUPDS* evaluated along the course of experimental evolution.

Source of variation		Type III Sum of squares	d.f.	Mean squares	*F*	P	η_P^2	1—β
A	Hypothesis	5.960	1	5.960	1255.393	< 0.001	0.962	1
	Error	0.236	49.783	0.005				
t	Hypothesis	3.705	1	3.705	337.122	< 0.001	0.399	1
	Error	5.583	508	0.011				
G	Hypothesis	1.299	9	0.144	31.668	< 0.001	0.868	1
	Error	0.197	43.293	0.005				
t × G	Hypothesis	0.144	9	0.016	1.458	0.161	0.025	0.700
	Error	5.583	508	0.011				
L(G)	Hypothesis	0.167	38	0.004	0.399	1	0.029	0.439
	Error	5.583	508	0.011				
t × L(G)	Hypothesis	0.224	37	0.006	0.550	0.986	0.039	0.609
	Error	5.583	508	0.011				

η_P^2: magnitude of the effect; 1—β: power of the test.
The different factors are defined in equation 1: *t* evolutionary passage; *G* plant genotype; *L* virus evolutionary lineage; *t* × *G* interaction between evolutionary passage and plant genotype; *L*(*G*) viral evolving lineage within-host genotype; and *t* × *L*(*G*) interaction between evolutionary passage and viral evolving lineage.

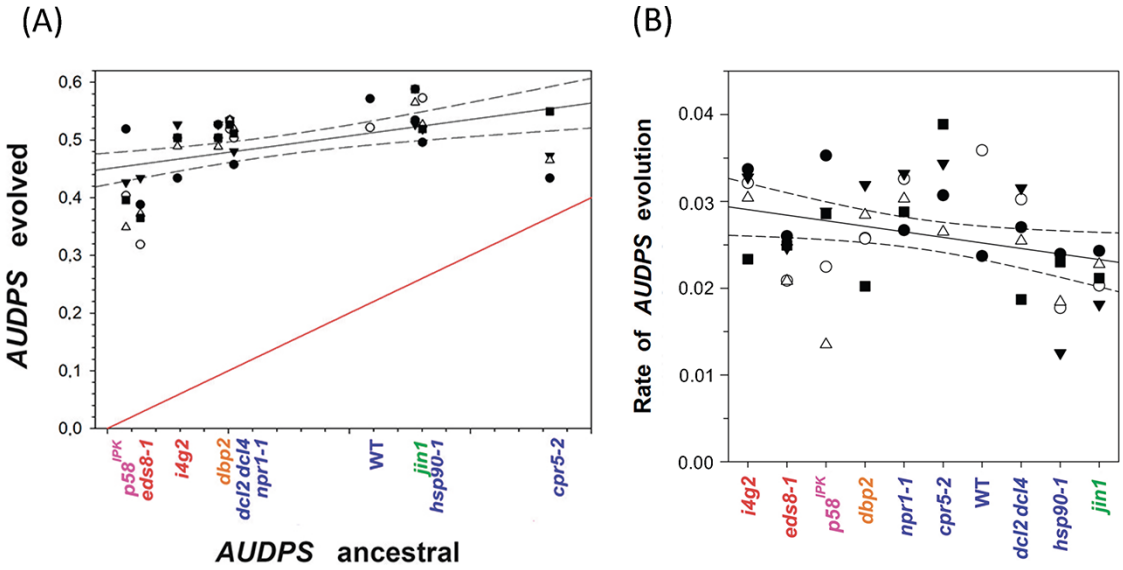

Figure 3. (A) Test of the contribution of historical contingency to the observed pattern of adaptation of TuMV to the different *A. thaliana* genotypes. The red line represents the null hypothesis of historical differences being fully preserved despite adaptation (i.e. ancestral and evolved values are exactly the same). (B) Estimated rates of evolution for *AUDPS* obtained from the fitting of Eq. 2 to the data shown in Fig. 2. *A. thaliana* genotypes are ranked from the less to the more permissive to TuMV infection according to phenogroups defined in Fig. 1. In both panels, different symbols represent different independent lineages evolved on the corresponding host genotype, solid lines represent the linear regression of the data and dashed lines the 95 per cent confidence intervals for the regression lines, and genotypes are colored according to phenogroups and using the same color palette than in Fig. 1

3.4 The degree of permissiveness of plant genotypes to infection drives the evolution of TuMV lineages into more or less specialization

To analyze the specificity of adaptation of each evolved TuMV lineage, we performed a full cross-infection experiment. In this experiment, the forty-four viral lineages evolved in the mutant genotypes (excluding the two WT-evolved lineages) were inoculated to ten plants of the nine *A. thaliana* mutant genotypes used in the evolution experiments (excluding WT plants). The presence of symptoms in each plant was recorded daily for up to 12 dpi. This dataset was analyzed using two different approaches, first an ANOVA-like that evaluates the effect of host genotypes, viral lineages, and their interactions (Schmid-Hempel 2011); and second, the inference of nestedness, modularity and specialization of a bipartite infection network (Weitz et al. 2013). Both approaches drive to identical conclusions. For the sake of keeping the presentation concise, the results of the first approach are provided in Supplementary Text S2 and Table S1.

For the second analytical approach, we used an infection matrix of forty-four rows (viral lineages evolved in each local host genotype) by nine columns (test genotypes). Fig. 4 shows the packed infection matrix with rows and columns organized to better highlight its nestedness and modularity (Weitz et al. 2013). The infection network was significantly nested (temperature nestedness: $T = 1.142$, $P < 0.001$), with genotypes *jin1* and *dcl2 dcl4* being permissive to most viral lineages (universally susceptible hosts), while the most restrictive genotypes *eds8-1* and $p58^{IPK}$ were more efficiently infected by lineages that were precisely evolved in these two genotypes. Likewise, the most generalist viral lineages were *eds8-1*/L4, $p58^{IPK}$/L3 and $p58^{IPK}$/L4 that infected the nine mutant host genotypes Fig. 4 with high efficiency (universally virulent viruses). On another hand, the most specialized viral lineages that were able to more efficiently infect only their local hosts, were all surviving lineages evolved in *cpr5-2*, four lineages evolved in *dcl2 dcl4* and four lineages evolved in *jin1* Fig. 4. Therefore, we conclude that more restrictive host genotypes tended to select for

	jin1	*dcl2 dcl4*	*cpr5-2*	*npr1-1*	*hsp90-1*	*dbp2*	*i4g2*	*p58*^{IPK}	*eds8-1*	*d'*
eds8-1/L4	6,9	6,3	6,2	6,7	6	6,3	5,95	4,5	4,3	0,006
p58^{IPK}/L3	6,9	4,9	6,5	6,1	5,7	6,5	5,8	3,7	4,1	0,008
p58^{IPK}/L4	6,5	5,5	6,3	6	6	6,3	5,3	4	4,4	0,015
dcl2 dcl4/L1	7,1	5,6	6	6,1	6,2	6,1	6,1	6,1	4,1	0,015
eds8-1/L3	6,5	6,3	6,4	6,7	6,3	6,4	5,8	4,2	5,1	0,021
eds8-1/L5	6,2	7	5,8	6,7	5,1	5,6	5,8	3,4	4	0,022
eds8-1/L1	6,6	6,3	6,8	4,7	4	4,6	4	4	4,6	0,031
p58^{IPK}/L5	6,1	7	5,9	6	4,9	5,8	5,3	5,1	3,1	0,032
p58^{IPK}/L2	6,9	5,1	6,1	4,1	4,9	4,7	4	4,7	3,3	0,033
eds8-1/L2	6,5	6,2	6,6	4,1	5,2	4,6	3,7	3,7	5	0,034
i4g2/L2	6,5	5,6	5,6	4,7	5,7	5,4	5,5	4,7	1,9	0,035
dbp2/L3	6,9	6,4	6,8	6,5	6,8	6,7	5,7	5,7	4,8	0,040
hsp90-1/L1	5,8	6	6,7	4	5,4	5,2	4	4,5	4,1	0,041
i4g2/L1	5,8	6,4	5,9	3,7	4,7	5,3	5,4	4,2	2,3	0,041
dbp2/L1	6,5	5,7	6,5	4,9	6,2	6,4	4,8	5	2,8	0,041
dbp2/L5	7,2	7,4	6,2	6,6	5,7	7,1	4,4	5,5	3	0,047
hsp90-1/L2	6,5	4,7	6,2	4,4	6,2	4,3	3,4	4,1	2,9	0,047
hsp90-1/L3	6,2	7,2	6	5,7	6,4	6,5	5	3,7	3,6	0,047
hsp90-1/L4	6,7	6,9	6,3	6	6,5	6	5,5	6	4,1	0,048
i4g2/L3	6,6	6,7	5,1	5,9	5,8	3,7	6,5	5,9	3,8	0,049
i4g2/L4	6,5	6,7	5,5	5,3	5,3	3,6	6,3	5,3	4	0,049
i4g2/L5	6,5	6,3	5,5	5,5	5,3	5,4	5,6	5,5	3,2	0,050
npr1-1/L1	6,7	5,6	6,2	6	5,3	5,3	4,5	5,4	3,6	0,050
npr1-1/L2	6,1	5,7	6	6	5,2	5,3	4,4	3,9	3	0,052
npr1-1/L4	7,1	6,3	6,9	6,6	5,7	6,1	4,9	4,5	3,7	0,055
p58^{IPK}/L1	6,9	5,2	5,8	4,6	4,5	4,7	4,2	5,4	3,5	0,056
dbp2/L4	6,6	7	6,3	6,4	6,1	6,7	5,3	4,3	4,9	0,058
hsp90-1/L5	6	6,4	5,5	5,1	6,4	5,8	5,5	4,6	2,5	0,060
jin1/L5	7,5	7,8	5,7	6,7	7,2	5,7	3,4	4,1	2,8	0,061
npr1-1/L3	7,1	6,4	6,5	7	5,4	6,7	5,2	5,1	3,7	0,064
npr1-1/L5	7,1	7,7	6,4	7,4	3,3	5,7	5,5	4,6	3,3	0,064
cpr5-2/L1	5,7	5,7	6,8	6,7	4,9	4,7	4,2	4,2	3,5	0,067
cpr5-2/L3	5,9	5,4	6,7	4,6	4,4	4,3	3,4	2,4	3,7	0,070
cpr5-2/L4	5,8	5,5	6,3	6,2	5	5,4	4,3	3	2,8	0,071
cpr5-2/L5	6,7	5,6	7,2	5,4	5,4	5,3	4,4	2,7	3,5	0,072
dbp2/L2	6,4	5,1	6,4	5,3	5,8	6,8	4,8	5,3	2,9	0,075
dcl2 dcl4/L2	6,6	7,6	6,8	5,4	5	5,4	4,6	5,2	2,4	0,076
dcl2 dcl4/L3	7	7,9	6,4	6,9	6,1	6,1	6	3,2	4,1	0,082
dcl2 dcl4/L4	5,4	7,3	5,3	6	5,8	4,4	6,3	3,6	4,4	0,092
dcl2 dcl4/L5	6,2	7,8	6,6	6,7	7,2	5,3	6,6	5,1	2,6	0,102
jin1/L1	7,1	5,6	6,1	4,3	4,8	3,9	3,4	4,1	3,3	0,109
jin1/L2	7,1	5,7	6,7	4,6	4,9	4,6	4	4,6	3,5	0,119
jin1/L3	7,1	5,8	6,5	6	6,2	4,3	4,6	5	2,5	0,132
jin1/L4	7	6,4	4,7	6,4	3,6	6,3	4,8	4,7	3,6	0,331

Figure 4. Analysis of the full cross-infection matrix. Packed matrix that highlights its nested structure, compatible with a gene-for-gene infection model. Last column shows the species-level specialization index ($d' = 0$ for most generalists and $d' = 1$ for most specialists). Evolved TuMV lineages are colored according to the phenogroup of their local host genotype according to the color palette used in Fig. 1.

more generalist viruses while more permissive host genotypes did so for more specialized viruses, in agreement with a gene-for-gene infection model (Weitz et al. 2013).

Next, we computed Blüthgen, Menzel, and Blüthgen (2006) specialization indexes for the packed matrix Fig. 4. Firstly, we evaluated the standardized species-level measure of partner diversity d'. d' (last column in Fig. 4) ranged from < 0.01 for the more generalist evolved lineages (*eds8*-1/L4, and *p58*^{IPK}/L3) to > 0.1 for the more specialist ones (*dcl2 dcl4*/L5 and *jin1*/L1–L4). Very interestingly, d' values show a strongly significant negative correlation with the rank order degree of permissiveness of each host genotype, *i.e.* the order in which hosts appear in the columns of Fig. 4

(Spearman $r = -0.807$, 42 d.f., $P < 0.001$). This correlation supports the notion that more specialized viral lineages exploit host resources of more permissive hosts better than the more generalist viral species. Secondly, we computed the network-level specialization index H_2', obtaining a value of $H_2' = 0.028$ (uncorrected $H_2 = 5.916$, $H'_{min} = 3.835$, $H'_{max} = 5.916$; $P < 0.001$), meaning that, overall, the binary infection network shows a degree of specialization. Most of the lineages were able of infect one or a few host genotypes, a result mainly driven by those lineages evolved in the less restrictive host genotypes.

Finally, we sought to explore the modularity of the infection network. In this context, a module will refer to an aggregated set of viral lineages and their hosts characterized by more interactions within the module than between modules (Newman 2006; Dormann and Strauss 2014), as expected for a mutation accumulation infection model (Weitz et al. 2013). We computed the Q modularity index, that ranges from zero, when the community has no more links within modules than expected by chance, to a maximum value of one. We found a small yet significant modularity ($Q = 0.066$, $P < 0.001$) in the infection matrix Fig. 4: genotypes with mutations affecting the same signaling pathway may be selecting for viral lineages with similar properties, thus being able to infect a subset of plant genotypes with equal efficiency. An alternative hypothesis may be parallel evolution of lineages evolved in the same host genotype; the most representative cases of this possibility are the lineages evolved in *cpr5-2*, *dcl2 dcl4* and *jin1*. To distinguish between these two hypotheses, we computed a reduced matrix averaging the observed *AUDPS* among lineages evolved in the same host genotype and transforming this nine-by-nine infection matrix into its corresponding packed binary matrix, as described above. If the reduced matrix still shows significant modularity, the first hypothesis will hold on, but if modularity vanishes then the alternative hypothesis will be more parsimonious. The reduced matrix was no longer modular ($Q = 0.029$, $P = 0.078$). This supports the notion that the observed modularity was driven by convergent phenotypic evolution of lineages evolved into the same host genotype rather than by common selective pressures owed to mutations in overlapping defense mechanism.

3.5 Genomic changes in evolved TuMV lineages

Finally, we have explored the genomic changes experienced by the TuMV evolved lineages. A total of 119 mutational events have been observed, affecting 73 nucleotide positions (Supplementary Fig. S3 and Table S2). No single mutation was shared between all five independent lineages propagated on a plant genotype and very few mutations were observed in more than two lineages. According to the type of nucleotide substitution, ninety-eight were transitions and twenty-one transversions. Regarding their effect on the protein sequence, thirty were synonymous and eighty-nine nonsynonymous. Interestingly, some mutations, including thirteen nonsynonymous and four synonymous, have been observed multiple times in independent lineages. As discussed in the Section 2.8, treating each lineage as an observation and each host genotype as a subpopulation, the average nucleotide diversity within-host genotypes, referred only to the seventy-three polymorphic sites, was $\pi_S = 0.067 \pm 0.007$. On the other hand, the nucleotide diversity for the entire sample was $\pi_T = 0.073 \pm 0.008$. Hence, the estimated interhost genotype nucleotide diversity was $\delta_{ST} = 0.006 \pm 0.003$ and the coefficient of nucleotide differentiation (Nei 1982) $N_{ST} = 0.081 \pm 0.039$, a value significantly greater than zero ($z = 2.077$, $P = 0.019$). Thus, we conclude that minor yet significant genetic differentiation has been generated among viral lineages replicating in different host genotypes.

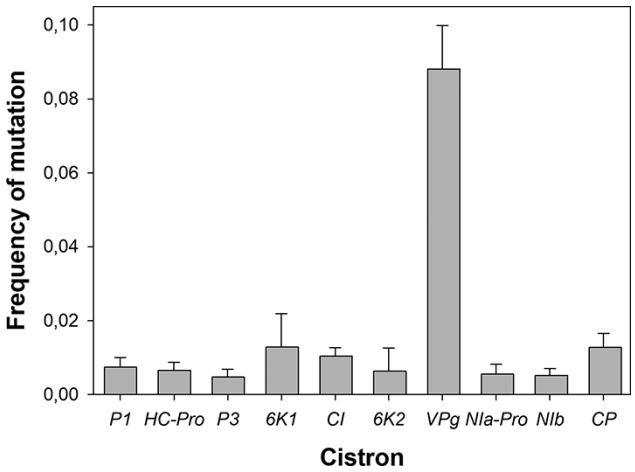

Figure 5. Frequency of mutations observed on each cistron. Error bars represent ±1 SEM.

To assess whether selection played a role in virus genetic differentiation among plant genotypes, we performed a Tajima's *D* test (Tajima 1989) and found that it was significantly negative ($D = -2.496$, $P = 0.006$). This result suggests the presence of selective sweeps acting on virus populations and presence of selection.

Next, we sought to characterize the distribution of mutational events along the nine nonoverlapping cistrons Fig. 5. The frequency of mutations per cistron, relative to the length of the corresponding cistron, was fitted to the logistic regression model shown in Eq. 4 in the Section 2.8. Highly significant differences exist ($\chi^2 = 143.206$, 9 d.f., $P < 0.001$) yet entirely due to the ~11-fold larger mutation frequency observed in the *VPg* cistron relative to the rest of the genome Fig. 5. Notice that all mutations observed in *VPg* are nonsynonymous and that all lineages except *eds8-1*/L3 carry at least one mutation in this cistron (Supplementary Fig. S3 and Table S2).

Convergent nonsynonymous mutations are, *a priori*, good candidates for adaptive mutations. Mutation CP/V148I appears in two lineages evolved in *cpr5-2* (Supplementary Fig. S3 and Table S2), mutation CP/S70N appear in lineage *dcl2 dcl4*/L1 and three lineages evolved in *jin1* (Supplementary Fig. S3 and Table S2), and two different mutations affecting CP; CP/D112G appears in lineage *npr1-1*/L4 and CP/D112A that appears in lineage *i4g2*/L5, that result in a similar replacement of side chains. In addition, ten nonsynonymous mutations in *VPg* are shared by several lineages (Supplementary Fig. S3 and Table S2). Out of these ten cases, three seem to be particularly promising candidates and are located in a narrow region of VPg (residues 113, 115, and 118) (Supplementary Fig. S3 and Table S1). Mutations G6237A, G6237C, A6238G, and U6239A all affect the same codon, resulting in amino acid replacements VPg/D113N, VPg/D113H, VPg/D113G, and VPg/D113E, respectively.

4. Discussion

4.1 Interaction between TuMV and different plant defenses

In this study we have explored the effect that mutations in different host disease signaling pathways or recessive resistance S genes have in the outcome of virus evolution. Our experimental pathosystem consisted of two well-studied components: the

model plant *A. thaliana* and TuMV, a virus with high prevalence in natural populations on this host (Pagán et al. 2010). Among the disease signaling pathways, we have studied genes involved in the SA, JA/ET pathways, and RNA-silencing; while among the S genes, we have included heat shock proteins, transcription factors, and components of the translation machinery. In a preliminary set of experiments, we compared phenotypic responses of different plant mutant genotypes to TuMV infection. Our results were, in some cases, at odds with the expected phenotypes for R genes, the most unexpected one being the result for *jin1*. *JASMONATE INSENSITIVE 1* (*JIN1*) is a negative regulator of SA-mediated defense responses, henceforth the mutant *jin1* has a constitutive expression of SAR (Laurie-Berry et al. 2006). Surprisingly, it turns out to be the most permissive genotype to TuMV infection, showing enhanced symptoms of disease (phenogroup G5). This may reflect the fact that the function of genes involved in disease signaling have been mostly defined in terms of plant interactions with biotrophic and necrotrophic bacteria and fungi but rarely in response to virus infections. Mutant genotypes only affecting components of the ISR pathway (e.g. *coi1-4*) behaved as WT plants in response to TuMV infection, thus confirming previous reports that ISR was inefficient against viral infections (Ton et al. 2002; Loebenstein 2009; Pieterse et al. 2009). However, mutant *eds8-1*, which avoids ISR but enhances SAR (Love et al. 2007) turned out to be among the most restrictive genotypes to infection (phenogroup G1). In agreement with our findings of a variable response to SA signaling, Singh et al. (2004) discussed examples of viruses in which SA-dependent responses to viral infection were strongly dependent on the virus used in the experiments. Replication of viruses such as alfalfa mosaic virus, potato virus X, or turnip vein clearing virus was inhibited by treating plants with SA, while cucumber mosaic virus appeared unaffected by the treatment and accumulated to normal levels.

The RNA-silencing pathway is considered as the main plant defense against viral pathogens (Voinnet 2001), with *DICER-LIKE 2* (*DCL2*) and *DICER-LIKE 4* (*DCL4*) encoding for the two dicer enzymes responsible for generating the 22- and 21-nucleotides long antiviral siRNAs. Therefore, the double mutant *dcl2 dcl4* was expected to be highly permissive to TuMV infection. However, infected plants were, overall, hardly distinguishable from the WT plants in their response to infection (Supplementary Figs. S2 and S3). A possible explanation would be the strong suppressor activity of HC-Pro in the WT plants that effectively counteracts the defense mechanisms (Kaschau and Carrington 2001). Indeed, it has been shown that the outcome of the interplay between plant RNA-silencing response and potyviruses is mostly driven by the efficiency of the viral HC-Pro suppression activity (Lin et al. 2007; Torres-Barceló et al. 2008).

The response to infection of genotypes carrying mutations in S genes was, in general, consistent with the *a priori* expectation. Mutant *i4g2* belonging to phenogroup G1, that is defective for the eIF4(iso)E factor, was highly restrictive to TuMV infection (Nicaise et al. 2007; Charron et al. 2008). Likewise, in agreement with previous descriptions, mutant *dbp2* belonging to phenogroup G3, was restrictive to potyvirus infection (Castelló et al. 2011). Finally, mutant *hsp90-1* showed a response to TuMV infection equivalent to WT plants, likely due to its functional redundancy with other heat shock proteins present in the cell that may be coopted by the virus to assist in their expected functions (Verchot 2012).

An interesting finding was the effect of the knocked down expression of gene *P58^{IPK}* on TuMV replication. In mammals P58^{IPK}, a tetratricopeptide-repeat containing protein, is recruited by viruses (e.g. influenza A virus) to inhibit interferon activation and cell death mediated by the dsRNA-activated protein kinase, thus favoring viral spread (Goodman et al. 2011). In our experiments, *p58^{IPK}* mutant plants showed enhanced tolerance to infection by showing weaker symptoms than WT plants despite achieving the same level of virus accumulation (Supplementary Fig. S1). In sharp contrast, Bilgin et al. (2003) found that infection of *p58^{IPK}*-silenced *N. benthamiana* and *A. thaliana* plants infected with tobacco mosaic virus led to death. Given the limited information available from other plant-virus pathosystems, additional experiments would be necessary to shed light into the potential antiviral role of this gene.

An important conclusion of our study, is that the generally accepted model of plant defense signaling pathways, mainly based on experiments done with bacteria and fungi, may not be most suitable to describe interaction between plants and viruses well. By contrast, recessive S gene-based resistance seems to better explain differences in susceptibility to infection and viral accumulation, thus being a more promising target for future development of resistant plants.

4.2. Evolution of more or less specialized viral strategies depends on the host genotype

The gene-for-gene and mutation accumulation models of host—virus interaction modes represent the two ends of a continuum of possible outcomes (Agrawal and Lively 2002). The most relevant difference between both models regards the expected genetic heterogeneity in both host and virus populations. With a pure gene-for-gene interaction, the susceptible host types are expected to disappear and the resistant types are expected to dominate the population. *Vice versa*, the most virulent virus allele would become fixed in the population at the cost of mild alleles. However, constitutive activation of defenses is known to be costly for *A. thaliana* [*e.g.* SA-related defense responses pay a fitness cost in absence of pathogens (Traw, Kniskern, and Bergelson 2007)] and high virulence usually comes with a cost in terms of pathogen's transmission (Acevedo et al. 2019). Hence, a pure gene-for-gene strategy seems unlikely to be achieved. By contrast, with a pure mutation accumulation interaction, negative frequency-dependent selection emerges, such that rare *A. thaliana* resistance alleles have advantage and, as a result, a genetic polymorphism shall be maintained (Schmid-Hempel 2011). Natural populations of *A. thaliana* contain considerable amount of genetic variability for tolerance (Pagán, Alonso-Blanco, and García-Arenal 2008) and for immunity-related genes (Todesco et al. 2010; Van de Weyer et al. 2019; Butković et al. 2021), thus suggesting that an arms race between pathogens and plants is still ongoing but it is unclear whether it may result in pure gene-for-gene or mutation accumulation interactions or lie somewhere in between. Evolution experiments with such different pathosystems, such as TuMV-*A. thaliana* (González, Butković, and Elena 2019), *Octosporea bayeri-Daphnia magna* (Altermatt and Ebert 2008), and *Serratia marcescens-Caenorhabditis elegans* (Gibson et al. 2020; White et al. 2020) have produced congruent results: parasites exposed to heterogeneous host populations evolved significantly lower virulence than parasites exposed to homogeneous host populations. However, a significant difference exists among pathosystems: while viruses exposed to genetically heterogenous host populations evolved as no-cost generalists, evolution of generalism in more complex parasites was constrained by a fitness tradeoff, as expected for the jack-of-all trades hypothesis (Bedhomme, Hillung, and Elena 2015).

Our results, as well as those by Hillung et al. (2014) and González, Butković, and Elena (2019) have shown the evolution of significantly nested bipartite infection networks, a finding compatible with the existence of a combination of specialist and generalist viruses and of more permissive and resistant host genotypes. Indeed, these studies have also shown that more permissive hosts selected for more specialized viruses while more restrictive hosts selected for more generalist viruses, here matching the predictions of the gene-for-gene model. Our observation of small yet significant modularity in the infection network was easily explained by convergent evolution of TuMV lineages evolved in the same host genotype. However, it has been recently shown in a long-term survey of the prevalence of different plant viruses in different hosts and habitats that nestedness and modularity in host-pathogen infection networks is possible due to the spatially patched distribution of habitats and temporal successions of plant species (Valverde et al. 2020): small spatial scales create modularity that coexist with global nestedness. This pattern may change spatially and temporally but remains stable over long evolutionary timescales.

4.3 Ancestral differences in TuMV performance across host genotypes have been almost completely erased after experimental evolution

A relevant question in evolutionary biology is the extent in which ancestral differences determine the fate of evolution. Put in other words, what are the relative contributions of adaptation, chance and historical contingency to the evolution of organismal fitness (Travisano et al. 1995). Two different situations can result. Firstly, ancestral differences among phenotypes are preserved during evolution despite a net increase in the mean trait values (due to selection) and differences among replicated lineages (due to chance; i.e. mutation and drift). Therefore, this situation would result in a nonzero slope in a regression of the evolved phenotypic values against the ancestral ones. The closer the slope is to one, the greater the importance of ancestral differences. Secondly, if ancestral trait variation was erased from the evolved populations because the combined effect of adaptation and chance, a regression slope smaller than one would be expected. The less effect of ancestral differences, the flatter the slope, being zero in the extreme case where ancestral differences have completely vanished. In our study, we found that ancestral differences in *AUDPS* were not entirely removed by the combined action of selection and chance. Some minor differences still are observable for lineages evolved in the most restrictive hosts $p58^{IPK}$ and *eds8-1* Fig. 3A.

4.4 Role of natural selection

We found evidence of significant genetic differentiation among TuMV lineages evolved in different plant genotypes. To test whether these differences were driven by selection we performed a Tajima's *D* test (Tajima 1989). The resulting negative *D* value was significant, that is compatible with the action of purifying selection, the presence of slightly deleterious mutations segregating in the populations or fast population expansions (Yang 2006). How to distinguish between these explanations? In independent fast expanding populations, many new mutations may be generated and they may rise in frequency in each population, thus being observed as singletons, mutations present in only one of the many coexisting genomes in each evolving TuMV lineage. Singletons inflate the number of segregating sites and thus cause $D<0$. Indeed, this is the case here: fifty-six out of the seventy-three observed variable sites are singletons, thus the observed pattern of molecular diversity among lineages evolved in the same host genotype and in different host genotypes is likely to be due to the exponential growth of viral populations within individual hosts.

However, we have found additional evidence supporting the action of positive selection: the existence of a number of convergent nonsynonymous mutations arising in independent lineages. Some of these nonsynonymous mutations evolved in the same host genotype but others arise in different host genotypes (Supplementary Fig. S3 and Table S2). Yet without a clear association with the particular signaling pathway, mutated *S* gene Table 1 or the phenogroup they belong to Fig. 1. Interestingly, most of these convergent mutations happened in the *VPg* cistron, that also turns out to be the most variable one Fig. 5. VPg plays many essential roles in genome transcription (it is linked to the 5′-end of the viral genome and provides the hydroxyl group that primes the synthesis of the complementary strains by the viral RdRp), translation [directly interacts with the eukaryotic initiation factors eIF(iso)4E and eIF(iso)4G], and interacts with all other viral proteins (Bosque et al. 2014) and some of the host cell proteins (Martínez et al. 2016, 2020). Indeed, in previous evolution experiments with potyviruses, *VPg* has also been shown to be an important target of selection. For example, Agudelo-Romero et al. (2008) found that a single amino acid replacement in VPg was enough to largely increase tobacco etch virus infectivity, severity of symptoms and viral load in *A. thaliana*. Similarly, Gallois et al. (2010) found that *A. thaliana* plants with knock-out mutations in the *eIF(iso)4E*, *eIF(iso)4G1* and *eIF(iso)4G2* genes were resistant to TuMV infection. Two mutations in the VPg (E116Q and N163Y) were enough to overcome this resistance and return to the original infection phenotype, although yeast-two hybrid assays showed that none of these mutations affected the binding of VPg with eIF(iso)4E (Gallois et al. 2010). As a final example, one of the most extensively used resistance genes against potato virus Y in commercial pepper cultivars is pvr^2, which has many different alleles (Nicaise et al. 2007; Charron et al. 2008). The pvr^2 locus encodes for the eIF4E factor that, as mentioned above, physically interacts with VPg. Interestingly, all the resistance-breaking viral isolates found so far contain mutations in the *VPg* cistron (Duprat et al. 2002; Moury et al. 2004; Ayme et al. 2006).

One of the two mutations identified by Gallois et al. (2010), VPg/E116Q, affects the same protein domain as mutations VPg/D113G and VPg/R118H identified here. We found VPg/D113G in several lineages evolved in different host genotypes, while VPg/R118H was only found in the *jin1* lineage. The mechanism by which these two mutations may confer a selective advantage to TuMV lineages cannot be inferred from our studies and will be the subject of a follow up paper.

4.5 Comparing these results with other pathosystems

Someone may wonder whether results reported here might reflect universal patterns of virus evolution on hosts with variable susceptibility to infection or just a particularity of the way plants deal with infections. Mongelli et al. (2022) performed very similar evolution experiments with drosophila C virus (DCV), also a picornavirus, infecting eight *Drosophila melanogaster* genotypes that carried mutations affecting innate immunity antiviral defense pathways. Firstly, Mongelli et al. (2022) have also observed that the extent and evolutionary dynamics of viral load and infectivity depended on the particular host genotype, with a clear tendency to increase viral load in immunity-deficient flies. Secondly, also in agreement with our observations, DCV results also highlight pleiotropy (viral genotype-by-host genotype interaction)

as a major determinant of viral evolution. Indeed, they clearly show that the fitness effect of mutations that already existed in the standing genetic variation of the stock DCV population was strongly dependent on both, the fly's genetic background (the same mutation being beneficial or deleterious in different backgrounds) and the virus' genetic background (epistatic interactions with other mutations in the same haplotype). Thirdly, our observation that ancestral phenotypic differences in virulence across host genotypes can be erased after a few passages in each host genotype are also in agreement with Mongelli et al. (2022) observations, which suggest that the more restrictive a host genotype is to infection the more changes of selection and evolution of generalist viruses.

To conclude, besides obvious differences among experimental systems and other subtleties, these two studies demonstrate that experimental evolution-based approaches can provide insightful information about the constraints imposed by different defense signaling pathways on virus evolution and remark the prevalence on some pathways over others in controlling not only virus replication and accumulation but also, more broadly interesting, virus evolution.

4.6 Concluding remarks

Since our evolution experiments all started with an *A. thaliana* naïve strain of TuMV, someone may consider as a potential weakness of our study the difficulty to disentangle between general adaptations to the plant host from specific adaptations to the different mutant genotypes. Although obviously some common factors are shared by all ten plant genotypes, they differ in a well-defined component (the mutated gene) that we have shown affects their permissiveness to infection. The fact that we have found significant differences in the outcome of the evolution experiments performed in different plant genotypes, by itself, is evidence that each host genotype represents a somehow different selective environment. Unfortunately, at this stage, it is not possible to assign an adaptive value to every mutation observed in the different lineages. Doing so would require to generate them individually and in all relevant combinations in the infectious clone p35STunos and test their effect on *AUDPS* across the ten host genotypes. Although doable, it is a tremendous task beyond the scope of this study. The best assessment we can do so far about adaptive values is the commonly assumed principle that convergent mutations rising in independent lineages evolved in the same host genotype must provide a host-specific fitness advantage.

Pathogens evolve to escape from host defense mechanisms. Understanding how different defense mechanisms constrain the pathogen evolution is key to understand the evolutionary dynamics of infectious diseases. Here we aimed to determine the impact of defects in host defense mechanisms on virus evolution. We observed that virus interaction with defective hosts resulted in different intensity of disease-related traits, intensity that was determined by the disrupted defensive mechanism. Virus evolution on hosts with different degree of permissiveness shows that: (1) viral rates of evolution depend on the specific defective defense mechanism of the host. (2) Viruses evolve as more generalists when evolving in hosts with stronger defenses. On the contrary, evolving in more permissive hosts results in more specialized viruses. (3) Evolution results in a reduction of ancestral genetic variation, which occurs independently of the host permissiveness. (4) Regardless of their host's defenses, evolved viruses showed convergent mutations on the same region of their genome. Altogether, this work describes the constrains that the degree of host immunity can impose on virus evolution.

Data availability

All raw data are available at https://git.csic.es/SFElena/tumv-evolution-in-a.-thaliana-genotypes-with-deficient-immune-responses.

Supplementary data

Supplementary data is available at *Virus Evolution* online.

Acknowledgements

We thank Francisca de la Iglesia and Paula Agudo for excellent technical assistance and the rest of the EvolSysVir lab members for fruitful discussions.

Funding

This work was supported by grants BFU2015-65037-P and PID2019-103998GB-I00 (Agencia Estatal de Investigación - FEDER) and PROMETEU2019/012 (Generalitat Valenciana) to S.F.E. and by Natural Science Foundation China grant 31872414 to B.W.

Conflict of interest: None declared.

References

Acevedo, M. A. et al. (2019) 'Virulence-driven Trade-offs in Disease Transmission: A Meta-analysis', *Evolution*, 73: 636–47.

Agrawal, A., and Lively, C. M. (2002) 'Infection Genetics: Gene-for-gene versus Matching-alleles Models and All Points in Between', *Evolutionary Ecology Research*, 4: 79–90.

Agudelo-Romero, P. et al. (2008) 'Virus Adaptation by Manipulation of Host's Gene Expression', *PLoS ONE*, 3: e2397.

Altermatt, F., and Ebert, D. (2008) 'Genetic Diversity of *Daphnia Magna* Populations Enhances Resistance to Parasites', *Ecology Letters*, 11: 918–28.

Altizer, S. et al. (2006) 'Seasonality and the Dynamics of Infectious Diseases', *Ecology Letters*, 9: 467–84.

Alves, K. S., and Del Ponte, E. M. (2021) 'Analysis and Simulation of Plant Disease Progress Curves in R: Introducing the *Epifitter* Package', *Phytopathology Research*, 3: 22.

Anttila, J. et al. (2015) 'Environmental Variation Generates Environmental Opportunist Pathogen Outbreaks', *PLoS ONE*, 10: e0145511.

Ayme, V. et al. (2006) 'Different Mutations in the Genome-linked Protein VPg of Potato Virus Y Confer Virulence on the *Pvr2*^{3} Resistance in Pepper', *Molecular Plant-Microbe Interactions*, 19: 557–63.

Bascompte, J. et al. (2003) 'The Nested Assembly of Plant-animal Mutualistic Networks', *Proceedings of the National Academy of Sciences of the USA*, 100: 9389–9387.

Bedhomme, S., Hillung, J., and Elena, S. F. (2015) 'Emerging Viruses: Why are Not Jacks of All Trades?', *Current Opinion in Virology*, 10: 1–6.

Bilgin, D. D. et al. (2003) '$P58^{IPK}$, a Plant Ortholog of Double-stranded RNA-dependent Protein Kinase PKR Inhibitor, Functions in Viral Pathogenesis', *Developmental Cell*, 4: 651–61.

Blüthgen, N., Menzel, F., and Blüthgen, N. (2006) 'Measuring specialization in species interaction networks', *BMC Ecology*, 6: 9.

Bosque, G. et al. (2014) 'Topology Analysis and Visualization of *Potyvirus* Protein-protein Interaction Network', *BMC Systems Biology*, 8: 129.

Bouché, N. et al. (2006) 'An Antagonistic Function for Arabidopsis DCL2 in Development and a New Function for DCL4 in Generating Viral siRNAs', *EMBO Journal*, 25: 3347–56.

Boyes, D. C. et al. (2001) 'Growth Stage-based Phenotypic Analysis of Arabidopsis: A Model for High Throughput Functional Genomics in Plants', *The Plant Cell*, 13: 1499–510.

Brown, J. K. M., and Tellier, A. (2011) 'Plant-parasite Coevolution: Bridging the Gap between Genetics and Ecology', *Annual Review of Phytopathology*, 49: 345–67.

Butković, A. et al. (2021) 'A Genome-wide Association Study Identifies *Arabidopsis Thaliana* Genes that Contribute to Differences in the Outcome of Infection with Two *Turnip Mosaic Potyvirus* Strains that Differ in Their Evolutionary History and Degree of Host Specialization', *Virus Evolution*, 7: veab063.

Cao, H. et al. (1994) 'Characterization of an Arabidopsis Mutant that Is Nonresponsive to Inducers of Systemic Acquired Resistance', *The Plant Cell*, 6: 1583–92.

Carr, J. P., Lewsey, M. G., and Palukaitis, P. (2010) 'Signaling in Induced Resistance', *Advances in Virus Research*, 76: 57–121.

Castelló, M. J. et al. (2011) 'A Plant Small Polypeptide Is A Novel Component of DNA-binding Protein Phosphatase 1-mediated Resistance to Plum Pox Virus in Arabidopsis', *Plant Physiology*, 157: 2206–15.

Cervera, H. et al. (2018) 'Viral Fitness Correlates with the Magnitude and Direction of the Perturbation Induced in the Host's Transcriptome: The *Tobacco Etch Potyvirus*-tobacco Case Study', *Molecular Biology and Evolution*, 35: 1599–615.

Charron, C. et al. (2008) 'Natural Variation and Functional Analyses Provide Evidence for Coevolution between Plant eIF4E and Potyviral VPg', *Plant Journal*, 54: 56–68.

Chen, C. C. et al. (2003) 'Identification of Turnip Mosaic Virus Isolates Causing Yellow Stripe and Spot on Calla Lily', *Plant Disease*, 87: 901–5.

Corrêa, R. L. et al. (2020) 'Viral Fitness Determines the Magnitude of Transcriptomic and Epigenomic Reprogramming of Defense Responses in Plants', *Molecular Biology and Evolution*, 37: 1866–81.

Cui, H. et al. (2018) 'Antagonism of Transcription Factor MYC2 by EDS1/PAD4 Complexes Bolsters Salicylic Acid Defense in Arabidopsis Effector-triggered Immunity', *Molecular Plant*, 11: 1053–66.

Dormann, C. F., and Strauss, R. (2014) 'A Method for Detecting Modules in Quantitative Bipartite Networks', *Methods in Ecology and Evolution*, 5: 9–98.

Duprat, A. et al. (2002) 'The Arabidopsis Eukaryotic Initiation Factor (Iso)4e Is Dispensable for Plant Growth but Required for Susceptibility to Potyviruses', *Plant Journal*, 32: 927–34.

Flor, H. H. (1956) 'The Complementary Genetic Systems in Flax and Flax Rush', *Advances in Genetics*, 8: 29–54.

Frank, S. A. (1993) 'Specificity *versus* Detectable Polymorphism in Host-parasite Genetics', *Proceedings of the Royal Society B: Biological Sciences*, 254: 191–7.

Gallois, J. L. et al. (2010) 'Single Amino Acid Changes in the Turnip Mosaic Virus Viral Genome-linked Protein (Vpg) Confer Virulence Towards *Arabidopsis Thaliana* Mutants Knocked Out for Eukaryotic Initiation Factors eIF(iso)4E and eIF(iso)4G', *Journal of General Virology*, 91: 288–93.

Gandon, S. (2004) 'Evolution of Multihost Parasites', *Evolution*, 58: 455–69.

Ganusov, V. V., Bergstrom, C. T., and Antia, R. (2002) 'Within-host Population Dynamics and the Evolution of Microparasites in a Heterogeneous Host Population', *Evolution*, 56: 213–23.

Gibson, A. K. et al. (2020) 'The Evolution of Parasite Host Range in Heterogeneous Host Populations', *Journal of Evolutionary Biology*, 33: 773–82.

González, R., Butković, A., and Elena, S. F. (2019) 'Role of Host Genetic Diversity for Susceptibility-to-infection in the Evolution of Virulence of a Plant Virus', *Virus Evolution*, 5: vez024.

Goodman, A. G. et al. (2011) 'Virus Infection Rapidly Activates the $P58^{IPK}$ Pathway, Delaying Peak Kinase Activation to Enhance Viral Replication', *Virology*, 417: 27–36.

Gupta, V., Willits, M. G., and Glazebrook, J. (2000) '*Arabidopsis thaliana EDS4* contributes to salicylic acid (SA)-dependent expression of defense responses: Evidence for inhibition of jasmonic acid signaling by SA', *Molecular Plant-Microbe Interactions*, 13: 503–11.

Haraguchi, Y., and Sasaki, A. (2000) 'The Evolution of Parasite Virulence and Transmission Rate in a Spatially Structured Population', *Journal of Theoretical Biology*, 203: 85–96.

Hillung, J. et al. (2014) 'Experimental Evolution of an Emerging Plant Virus in Host Genotypes that Differ in Their Susceptibility to Infection', *Evolution*, 68: 2467–80.

Hughes, W. H. O., and Boomsma, J. J. (2006) 'Does Genetic Diversity Hinder Parasite Evolution in Social Insect Colonies?', *Journal of Evolutionary Biology*, 19: 132–43.

Jeger, M. J., and Viljanen-Rollinson, S. (2001) 'The Use of the Area under the Disease-progress Curve (AUDPC) to Assess Quantitative Disease Resistance in Crop Cultivars', *Theoretical and Applied Genetics*, 102: 32–40.

Kachroo, P., Chandra-Shekara, A. C., and Klessig, D. F. (2006) 'Plant Signal Transduction and Defense against Viral Pathogens', *Advances in Virus Research*, 66: 161–91.

Kaschau, K., and Carrington, J. C. (2001) 'Long-distance Movement and Replication Maintenance Functions Correlate with Silencing Suppression Activity of Potyviral HC-Pro', *Virology*, 285: 71–81.

Kimura, M. (1980) 'A Simple Method for Estimating Evolutionary Rate of Base Substitutions through Comparative Studies of Nucleotide Sequences', *Journal of Molecular Evolution*, 16: 111–20.

Laurie-Berry, N. et al. (2006) 'The *Arabidopsis Thaliana JASMONATE INSENSITIVE 1* Gene Is Required for Suppression of Salicylic Acid-dependent Defenses during Infection by *Pseudomonas Syringae*', *Molecular Plant-Microbe Interactions*, 19: 789–800.

Lin, S. S. et al. (2007) 'Modifications of the Helper Component-protease of Zucchini Yellow Mosaic Virus for Generation of Attenuated Mutants for Cross Protection against Severe Infection', *Phytopathology*, 97: 287–96.

Lively, C. M. (2010) 'The Effect of Host Genetic Diversity on Disease Spread', *American Naturalist*, 175: e149–52.

Loebenstein, G. (2009) 'Local Lesions and Induced Resistance', *Advances in Virus Research*, 75: 73–117.

Love, A. J. et al. (2007) 'Components of Arabidopsis Defense- and Ethylene-signaling Pathways Regulate Susceptibility to Cauliflower Mosaic Virus by Restricting Long-distance Movement', *Molecular Plant-Microbe Interactions*, 20: 659–70.

Mäkinen, K. (2019) 'Plant Susceptibility Genes as a Source for Potyvirus Resistance', *Annals of Applied Biology*, 173: 122–9.

Mariani, M. S. et al. (2019) 'Nestedness in Complex Networks: Observation, Emergence, and Implications', *Physics Reports*, 813: 1–90.

Martínez, F. et al. (2016) 'Interaction Network of *Tobacco Etch Potyvirus* NIa Protein with the Host Proteome during Infection', *BMC Genomics*, 17: 1.

——— et al. (2020) 'A Comprehensive Physical Interaction Map between the *Turnip Mosaic Potyvirus* and *Arabidopsis Thaliana* Proteomes', *Research Square*.

Mine, A. et al. (2017) 'An Incoherent Feed-forward Loop Mediates Robustness and Tunability in a Plant Immune Network', *EMBO Reports*, 18: 464–76.

Mongelli, V. et al. (2022) 'Innate Immune Pathways Act Synergistically to Constrain RNA Virus Evolution in *Drosophila Melanogaster*', *Nature Ecology and Evolution*, 6: 565–78.

Moreno-Gámez, S., Stephan, W., and Tellier, L. (2013) 'Effect of Disease Prevalence and Spatial Heterogeneity on Polymorphism

Maintenance in Host-parasite Interactions', *Plant Pathology*, 62: 133–41.

Moury, B. et al. (2021) 'The Quasi-universality of Nestedness in the Structure of Quantitative Plant-parasite Interactions', *Peer Community Journal*, 1: e44.

——— et al. (2004) 'Mutations in Potato Virus Y Genome-linked Protein Determine Virulence Towards Recessive Resistances in *Capsicum Annuum* and *Lycopersicon Hirsutum*', *Molecular Plant-Microbe Interaction*, 17: 322–9.

Nawrath, C. et al. (2002) '*EDS5*, an Essential Component of Salicylic Acid-dependent Signaling for Disease Resistance in Arabidopsis, Is a Member of the MATE Transporter Family', *The Plant Cell*, 14: 275–86.

Nawrath, C., and Métraux, J. P. (1999) 'Salicylic Acid Induction-deficient Mutants of Arabidopsis Express PR-2 and PR-5 and Accumulate High Levels of Camalexin after Pathogen Inoculation', *The Plant Cell*, 11: 1393–404.

Nei, M. (1982) 'Evolution of Human Races at the Gene Level'. In: Bonné-Tamir, B. (ed.) *Human Genetics, Part A: The Unfolding Genome*. New York: Alan R. Liss. 167–81.

Newman, M. E. J. (2006) 'Modularity and Community Structure in Networks', *Proceedings of the National Academy of Sciences of the USA*, 103: 8577–82.

Nicaise, V. et al. (2007) 'Coordinated and Selective Recruitment of eIF4E and eIF4G Factors for Potyvirus Infection in *Arabidopsis Thaliana*', *FEBS Letters*, 581: 1041–6.

Pagán, I., Alonso-Blanco, C., and García-Arenal, F. (2008) 'Host Responses in Life-history Traits and Tolerance to Virus Infection in *Arabidopsis Thaliana*', *PLoS Pathogens*, 4: e1000124.

Pagán, I. et al. (2010) '*Arabidopsis thaliana* as a model for the study of plant-virus Co-evolution', *Philosophical Transactions of the Royal Society B*', *Biological Sciences*, 365: 1983–95.

Parrat, S. R., Numminen, E., and Laine, A. L. (2016) 'Infectious Disease Dynamics in Heterogeneous Landscapes', *Annual Review of Ecology, Evolution, and Systematics*, 47: 283–306.

Pfenning, K. (2001) 'Evolution of Pathogen Virulence: The Role of Variation in Host Phenotype', *Proceedings of the Royal Society B Biological Sciences*, 268: 755–60.

Pieterse, C. M. J. et al. (2009) 'Networking by Small-molecule Hormones in Plant Immunity', *Nature Chemical Biology*, 5: 308–16.

——— et al. (2012) 'Hormonal Modulation of Plant Immunity', *Annual Review of Cellular and Developmental Biology*, 28: 489–521.

Regoes, R. R., Nowak, M. A., and Bonhoeffer, S. (2000) 'Evolution of Virulence in a Heterogeneous Host Population', *Evolution*, 54: 64–71.

Rodríguez, D., and Torres-Sorando, L. (2001) 'Models of Infectious Diseases in Spatially Heterogeneous Environments', *Bulletin of Mathematical Biology*, 63: 547–71.

Rozas, J. et al. (2017) 'DnaSP 6: DNA Sequence Polymorphism Analysis of Large Data Sets', *Molecular Biology and Evolution*, 34: 3299–302.

RStudio Team (2020) RStudio: Integrated Development for R. Boston, MA: RStudio, PBC..

Sallinen, S. et al. (2020) 'Intraspecific Host Variation Plays a Key Role in Virus Community Assembly', *Nature Communications*, 11: 5610.

Schmid-Hempel, P. (2013) 'Host-parasite genetics'. In: Oxford University Press (ed) *Evolutionary Parasitology: The Integrated Study of Infections, Inmunology, Ecology, and Genetics*. Chapter 10. pp. 259–72. Oxford, UK.

Schmid-Hempel, P., and Koella, J. C. (1994) 'Variability and Its Implications for Host-parasite Interactions', *Parasitology Today*, 10: 98–102.

Simko, I., and Piepho, H. P. (2012) 'The Area under the Disease Progress Stair: Calculation, Advantage, and Application', *Phytopathology*, 102: 381–9.

Singh, D. P. et al. (2004) 'Activation of Multiple Antiviral Defence Mechanisms by Salicylic Acid', *Molecular Plant Pathology*, 5: 57–63.

Soosaar, J. L. M., Burch-Smith, T. M., and Dinesh-Kumar, S. P. (2005) 'Mechanisms of Plant Resistance to Viruses', *Nature Reviews: Microbiology*, 3: 789–99.

Tajima, F. (1989) 'Statistical Methods for Testing the Neutral Mutation Hypothesis by DNA Polymorphism', *Genetics*, 123: 585–95.

Tamura, K., Stecher, G., and Kumar, S. (2021) 'Molecular Evolutionary Genetics Analysis Version 11', *Molecular Biology and Evolution*, 38: 3022–7.

Thines, B. et al. (2007) 'JAZ Repressor Proteins are Targets of the SCF(COI1) Complex during Jasmonate Signalling', *Nature*, 448: 661–5.

Todesco, M. et al. (2010) 'Natural Allelic Variation Underlying a Major Fitness Trade-off in *Arabidopsis Thaliana*', *Nature*, 465: 632–6.

Ton, J. et al. (2002) 'Differential Effectiveness of Salicylate-dependent and Jasmonate/ethylene-dependent Induced Resistance in Arabidopsis', *Molecular Plant-Microbe Interactions*, 15: 27–34.

Torres-Barceló, C. et al. (2008) 'From Hypo- to Hypersuppression: Effect of Amino Acid Substitutions on the RNA-silencing Suppressor Activity of the *Tobacco Etch Potyvirus* HC-Pro', *Genetics*, 180: 1039–49.

Travisano, M. et al. (1995) 'Experimental Tests of the Roles of Adaptation, Chance, and History in Evolution', *Science*, 267: 87–90.

Traw, M. B., Kniskern, J. M., and Bergelson, J. (2007) 'SAR Increases Fitness of *Arabidopsis Thaliana* in the Presence of Natural Bacterial Pathogens', *Evolution*, 61: 2444–9.

Valverde, S. et al. (2020) 'Coexistence of Nestedness and Modularity in Host-pathogen Infection Networks', *Nature Ecology and Evolution*, 4: 568–77.

Van de Weyer, A. L. et al. (2019) 'A Species-wide Inventory of NLR Genes and Alleles in *Arabidopsis Thaliana*', *Cell*, 178: 1260–72.

Van Wees, S. C. M. et al. (2000) 'Enhancement of Induced Disease Resistance by Simultaneous Activation of Salicylate- and Jasmonate-dependent Defense Pathways in *Arabidopsis Thaliana*', *Proceedings of the National Academy of Sciences of the USA*, 97: 8711–6.

Verchot, J. (2012) 'Cellular Chaperones and Folding Enzymes are Vital Contributors to Membrane Bound Replication and Movement Complexes during Plant RNA Virus Infection', *Frontiers in Plant Sciences*, 3: 271.

Voinnet, O. (2001) 'RNA Silencing as a Plant Immune System against Viruses', *Trends in Genetics*, 17: 449–59.

Weitz, J. S. et al. (2013) 'Phage-bacteria Infection Networks', *Trends in Microbiology*, 21: 82–91.

White, P. S. et al. (2020) 'Host Heterogeneity Mitigates Virulence Evolution', *Biology Letters*, 16: 20190744.

Wiser, M., Ribeck, N., and Lenski, R. E. (2013) 'Long-term Dynamics of Adaptation in Asexual Populations', *Science*, 342: 1364–7.

Yang, Z. (2006) *Computational Molecular Evolution*. UK: Oxford University Press, Oxford. pp. 262–4.

——— et al. (2020) 'Jasmonate Signaling Enhances RNA Silencing and Antiviral Defense in Rice', *Cell Host & Microbe*, 28: 89–103.

Zhou, J. M., and Zhang, Y. (2020) 'Plant Immunity: Danger Perception and Signaling', *Cell*, 181: 978–89.